


# Solitary Neurofibroma Of The Spermatic Cord: A Case Report

José Boto<sup>1\*</sup>, Sana Boudabbous<sup>1</sup>, Johannes Alexander Lobrinus<sup>2</sup>, Jolanta Gourmaud<sup>2</sup>, Sylvain Terraz<sup>1</sup>

1. Department of Radiology, Geneva University Hospital, Geneva, Switzerland

2. Department of Clinical Pathology, University Medical Center, Geneva, Switzerland

\* Correspondence: José Boto, Department of Radiology, Geneva University Hospital, Rue Gabrielle-Perret-Gentil 4, 1205 Genève, Switzerland

 Jose.M.BaiaoBoto@hcuge.ch

Radiology Case. 2015 Jun; 9(6):19-28 :: DOI: 10.3941/jrcr.v9i6.2206

## ABSTRACT

We report the ultrasound, computerized tomography, positron emission tomography and magnetic resonance imaging findings of a 38-year-old man with a biopsy proven solitary neurofibroma of the spermatic cord. Solitary neurofibromas of the male genital tract are exceedingly rare benign peripheral nerve sheath neoplasms composed of Schwann cells and fibroblasts. In contrast to schwannomas they are not bound by a capsule thus allowing infiltration between the nerve fascicles. Although they are benign lesions whose potential for malignant degeneration is very low, especially in the absence of neurofibromatosis type 1, accurate diagnosis is important as neurofibromas in this location can cause significant morbidity and psychological distress. Despite the extensive differential diagnosis of masses in the male inguinal canal, including both benign and malignant entities, a diagnosis of benign peripheral nerve sheath tumor can be potentially suggested based on imaging, particularly if MRI is performed. Surgical resection is the treatment of choice and the final diagnosis should be provided by histopathology, as was the case with this patient.

## CASE REPORT

### CASE REPORT

A 38 year-old man presented with discomfort in the right groin of a few weeks duration. An ultrasound (US) examination revealed bilateral inguinal hernias and a solitary well demarcated hypoechoic homogeneous mass in the right inguinal canal measuring 30 x 22 x 22 mm. The mass was richly vascularized and was in contact with the right iliac vessels (Fig. 1).

A multidetector computed tomography (MDCT) scan and a positron emission tomography-computed tomography (PET-CT) scan confirmed the presence of a solitary mass in the right spermatic cord with heterogeneous enhancement and moderate

uptake of 2-deoxy-2-(18F)fluoro-D-glucose (18F-FDG) (Fig. 2). No distant lesions were demonstrated.

Magnetic resonance imaging (MRI) of the pelvis revealed a well demarcated and relatively homogeneous mass in the right spermatic cord. The mass was isointense to muscle on T1-weighted imaging (T1WI), hyperintense on T2-weighted imaging (T2WI) and showed avid and uniform enhancement after injection of gadolinium contrast media (Fig. 3). There was no diffusion restriction (Fig. 4).

The patient subsequently underwent surgical resection of the mass by right inguinoscopy, and bilateral inguinal hernia repair in the same instance. A preliminary assessment of the

surgical specimen revealed a 40 x 40 mm mass of gelatinous consistency. Macroscopic histopathology showed a 40 x 36 x 23 mm well defined nodular tissue fragment weighing 13g (Fig. 5). Microscopically, the lesion consisted of multiple elongated cells with uniform oval nuclei for the most part, arranged in a lax richly vascularized fibrillary stroma (Fig. 6). Cellularity was more prominent in the central part of the lesion where Verocay bodies and a palisade-type of cellular arrangement were identified, which are typical features of schwannoma. No mitotic activity was found. Moreover, the lesion insinuated itself into the surrounding fibrofatty tissue without destroying it. Immunohistochemistry revealed expression of the S-100 protein by the tumor cells (Fig. 6). The histopathology diagnosis was benign neurofibroma with schwannoma-like elements centrally.

The patient showed good recovery from surgery at a one month follow-up visit. However, discovery of a relatively large neurofibroma in a young man generated suspicion of neurofibromatosis type 1 (NF1). A subsequent dermatology assessment revealed an isolated 9 x 4 cm "café au lait" spot on the posterior aspect of the right thigh but no cutaneous or plexiform neurofibromas, axillary or inguinal freckling, or Lisch nodules. NF1 was therefore deemed very unlikely.

## DISCUSSION

### Etiology & Demographics

Neurofibromas are benign peripheral nerve sheath neoplasms composed of Schwann cells and fibroblasts. They contain a rich network of collagen fibers and in contrast to schwannomas they are not bound by a capsule thus allowing infiltration between the nerve fascicles. On immunohistochemistry studies, neurofibromas express the S-100 protein. There are three types of neurofibromas: localized, diffuse and plexiform. The former is a well demarcated mass, whereas the latter presents as a diffusely infiltrating lesion along the course of a nerve and is pathognomonic of NF1. Diffuse neurofibromas occur most frequently in the subcutaneous soft tissues of the head and neck of children and young adults. Localized neurofibromas are the most common (90%) and the majority are solitary lesions not associated with NF1 [1]. In fact only 10% of patients with solitary neurofibromas have NF1 [2]. They occur equally in men and women and mostly in young patients (20-30 years) [2].

Although, most solitary neurofibromas are not associated with neurofibromatosis type 1 [1], a solitary neurofibroma of the spermatic cord could potentially occur in NF1 and be the only clinical finding. This is described as the "forme fruste" of NF1 [3]. Solitary neurofibromas of the spermatic cord arise from the genitofemoral or ilioinguinal nerve and are exceedingly rare lesions. Given the rarity of solitary neurofibromas of the male genital tract, a meaningful demographic analysis is difficult to carry out. To our knowledge, only 14 cases of solitary neurofibromas of the male genital tract have been described in the literature [4-17] (Table 1). Of these, only nine were actually neurofibromas of

the spermatic cord, with five being intrascrotal [5,6,8,10,16]. The age of the patients ranged from 8 to 86 (mean 49.5).

### Clinical & Imaging findings

Neurofibromas of the spermatic cord may present as a palpable mass, dull aching pain, or sensory loss [18]. In our case, the presentation was a palpable mass in the right groin associated with discomfort. From the literature reviewed, only two out of the 14 cases reported presented with pain [9,14]. Severe motor weakness is not a feature of neurofibromas of the spermatic cord and is usually observed with malignant tumors [18]. Other clinical signs of malignant transformation include pain and rapid growth [19]. Benign neurofibromas are usually smaller than 5 cm at presentation, whereas neurofibromas which have undergone malignant degeneration are frequently larger [2].

On US, solitary neurofibromas usually appear as well defined, relatively homogeneous, predominantly hypoechoic masses with poor to moderate vascularization on color and power Doppler. Some variability has nevertheless been observed with some solitary neurofibromas presenting as heterogeneous masses and showing posterior acoustic shadowing [20]. On non-contrast MDCT, they may appear as well demarcated masses with attenuation equivalent to skeletal muscle [20-30 hounsfield units (HU)] that enhance after administration of iodinated contrast media (CM) [21]. Enhancement is more pronounced in larger lesions [2]. On PET-CT, benign neurofibromas do not usually show increased uptake of the 18F-FDG radiotracer in keeping with their benign nature. A high standardized uptake value (SUV) may however be observed in case of malignant degeneration. Benign nerve sheath tumors may nevertheless show mildly increased 18F-FDG uptake, but uptake in malignant nerve sheath tumors is significantly higher (mean maximum SUV 8.5 versus 1.5, respectively) [22]. MRI is the modality of choice for the characterization of neurofibromas as it allows exquisite anatomical analysis of the lesion and its relation to the surrounding soft tissues as well as assessment of its enhancement dynamics and internal water diffusion restriction properties. This in turn enables characterization of the lesion as benign or malignant with a high degree of certainty. On MRI, neurofibromas usually appear as a mass which is isointense on T1WI and hyperintense on T2WI in relation to muscle [2]. However, a hyperintense rim and central area of low signal ("target sign") may also be seen on T2WI, which is thought to be due to a central area of collagenous stroma of increased density and condensed Schwann cells [2]. This sign is highly suggestive of neurofibroma, but may also be observed in schwannomas and malignant peripheral nerve sheath tumors [2]. Imaging signs of malignant transformation on MRI include T2WI heterogeneity and absence of the target sign [21]. Other signs of malignant degeneration include rapid increase in size, heterogeneity also on T1WI, intralesional hemorrhage or necrosis and peripheral enhancement [23-26]. The pattern of enhancement varies in benign and malignant peripheral nerve sheath tumors. In most cases, malignant lesions show increased heterogeneous enhancement, which is typically nodular and peripheral [27]. This is due to the presence of intratumoral hemorrhage and necrosis in malignant lesions [26]. Lesions that demonstrate the target sign typically

enhance more avidly in the central region [27]. Diffusion-weighted imaging (DWI) in correlation with the apparent diffusion coefficient (ADC) map of peripheral nerve sheath tumors has also proved useful in characterizing these lesions as benign or malignant with the latter showing low water diffusivity values [28].

#### Treatment & Prognosis

Solitary neurofibromas which are not associated with NF1 are usually treated by surgical excision. However, as they are unencapsulated and infiltrate between the nerve fascicles, sacrifice of the parent nerve is necessary. This is why conservative treatment or incomplete excision are preferred in deep seated lesions or those occurring in important nerves in order to minimize neurological injury and permanent damage [2].

The prognosis of solitary neurofibromas is usually excellent. Malignant degeneration is very rare in the absence of NF1 and only 4% in NF1 patients [2]. Local recurrence is uncommon in lesions not associated with NF1 [1].

#### Differential Diagnosis

The differential diagnosis of a mass in the male inguinal canal is relatively vast and for the most part comprising benign lesions or herniation of normal anatomical structures such as bowel hernias. Benign masses of the inguinal canal in men include lipoma, hematoma, abscess and desmoid tumor of the spermatic cord. Malignant processes of the male inguinal region include liposarcoma, Burkitt lymphoma, testicular carcinoma, sarcoma, and metastases [21]. All of these benign and malignant entities are more common than solitary neurofibroma.

Lipomas are usually obvious lesions on imaging, especially on MDCT and MRI as they have the same appearance as subcutaneous fat. Differentiation from liposarcoma may however be challenging, especially if the latter is well differentiated, in which case it will appear as a mass of fat attenuation and intensity on MDCT and MRI, respectively. Hematomas of the inguinal canal occur mainly as a result of trauma and/or anticoagulation therapy, and the diagnosis should be readily apparent based on the history and the typical imaging appearance of blood. The same applies to an abscess of the inguinal canal which can be secondary to an incarcerated and/or perforated hernia, diverticulitis or Meckel diverticulum and is accompanied by a typical clinical scenario including groin pain, fever and raised inflammatory markers. Desmoid tumors are associated with Gardner syndrome, familial adenomatous polyposis, and surgical scars [29]. Differentiation from neurofibroma may be difficult as desmoid tumors show low attenuation on MDCT, are hypointense on T1WI, and enhance after administration of contrast media. However, low or heterogeneous signal intensity on T2WI should enable differentiation from neurofibroma [21]. Burkitt lymphoma is a high-grade form of non-Hodgkin lymphoma which presents as heterogeneous enhancement of the spermatic cord [21] as opposed to the well defined nature of solitary neurofibromas. Testicular carcinoma is a relatively uncommon malignancy in men that spreads to the spermatic cord by hematogenous dissemination or direct invasion. Identification

of an intratesticular mass on ultrasound imaging in a patient should promptly suggest the diagnosis of testicular cancer, especially if associated with retroperitoneal lymphadenopathy on MDCT. Sarcoma of the inguinal canal is a rare tumor that presents as a firm, palpable mass that despite its nonspecific imaging appearance should not be mistaken for a benign process given its invasive nature, often extending into the abdomen [21].

The most common primaries associated with metastases to the inguinal canal are alveolar rhabdomyosarcoma and monophasic sarcoma, prostate cancer, Wilms tumor, carcinoid tumor, melanoma, and pancreatic cancer. In a patient with a known malignancy, a mass in the inguinal canal is considered a metastasis until proven otherwise, and indicates stage 4 disease if peritoneal carcinomatosis is absent [21].

#### TEACHING POINT

Solitary neurofibroma needs to be considered in the differential diagnosis of a mass of the male inguinal canal despite the extreme rarity of this entity. MRI is the modality of choice to confirm the presence and to characterize a tumor in this location due to its ability to exquisitely depict soft tissues and its multiplanar capabilities. Since malignant degeneration of solitary neurofibromas and local recurrence after resection are extremely rare in the absence of NF1, surgical management is curative.

#### REFERENCES

1. Murphey MD, Smith WS, Smith SE, Kransdorf MJ, Temple HT. From the archives of the AFIP. Imaging of musculoskeletal neurogenic tumors: radiologic-pathologic correlation. *Radiographics* 1999;19(5):1253-80. PMID: 10489179
2. Stoller D, Tirman P, Bredella M. *Diagnostic Imaging: Orthopedics*. First Edition. 2004 Amirsys. Salt Lake City, Utah, USA, pp 9.30-9.32
3. Jepson PM. Von Recklinghausen's disease presenting as a scrotal tumor. *Urology* 1975;5(2):270-274. PMID: 803732
4. Schulte TL, McDonald JR, Priestley JT. Tumors of the spermatic cord: Report of a case of neurofibroma. *J Am Med Assoc* 1939;112:2405
5. Levant B, Chetlin MA. Neurofibroma of the tunica albuginea testis. *J Urol* 1948;59(6):1187-1189. PMID: 18858064
6. Livolsi VA, Schiff M. Myxoid neurofibroma of the testis. *J Urol* 1948; 118(2):341-342. PMID: 894827

7. Johnson DE, Kaesler KE, Mackay BM, Ayala AG. Neurofibroma of the spermatic cord. *Urology* 1975;5(5):680-683. PMID: 1168964
8. Yamamoto M, Miyake K, Mitsuya H. Intrascrotal extratesticular neurofibroma. *Urology* 1982;20(2):200-201. PMID: 7112834
9. Sánchez-Chapado M, Aranda-Lassa JM, Caballero-Gómez M. Tumores de cordón: Apotación de un neurofibroma. *Arch Esp Urol* 1988;41(1):23-26. PMID: 3369887
10. Yoshimura K, Maeda O, Saiki S, Kuroda M, Miki T, Usami M, Kotake T. Solitary neurofibroma of the scrotum. *J Urol* 1990;143:823. PMID: 2313818
11. Issa M, Yagol R, Tsang D. Intrascrotal neurofibromas. *Urology* 1993;41(4):350-352. PMID: 8470322
12. Pellice C, Cosme M, Casalots J. Schwannoma des cordón espermático. *Actas Urol Esp* 1994;18(4):328-330. PMID: 7976725
13. Deliveliotis C, Albanis S, Skolarikos A, Varkarakis J, Protogerou V, Tamvakis N, Alargof E. Solitary neurofibroma of the spermatic cord. *Int Urol Nephrol* 2002;34(3):373-375. PMID: 12899231
14. Milathianakis KN, Karamanolakis DK, Mpogdanos IM, Trihia-Spyrou EI. Solitary neurofibroma of the spermatic cord. *Urol Int* 2004;72(3):271-274. PMID: 15084777
15. Türkyilmaz Z, Sönmez K, Karabulut R, Dursun A, Işık I, Ba?aklar C, Kale N, Gupta. A childhood case of intrascrotal neurofibroma with a brief review of the literature. *J Pediatr Surg* 2004;39(8):1261-1263. PMID: 15300541
16. Gupta S, Gupta R, Singh S, Pant L. Solitary intrascrotal neurofibroma: a case diagnosed on aspiration cytology. *Diagn Cytopathol*. 2011;39(11):843-846. PMID: 21994196
17. Hosseini MM, Geramizadeh B, Shakeri S, Karimi MH. Intrascrotal solitary neurofibroma: A case report and review of the literature. *Urol Ann* 2012;4(2):119-121. PMID: 22629013
18. Ogose A, Hotta T, Morita T, Higuchi T, Umezumi H, Imaizumi S, Hatano H, Kawashima H, Gu W, Endo N. Diagnosis of peripheral nerve sheath tumors around the pelvis. *Jpn J Clin Oncol*. 2004;34(7):405-413. PMID: 15342668
19. Bhargava R, Parham DM, Lasater OE, Chari RS, Chen G, Fletcher BD. MR imaging differentiation of benign and malignant peripheral nerve sheath tumors: use of the target sign. *Pediatr Radiol* 1997;27:124-129. PMID: 9028843
20. Reynolds DL Jr, Jacobson JA, Inampudi P, Jamadar DA, Ebrahim FS, Hayes CW. Sonographic characteristics of peripheral nerve sheath tumors. *AJR Am J Roentgenol*. 2004 Mar;182(3):741-4. PMID: 14975979
21. Bhosale PR, Patnama M, Viswanathan C, Szklaruk J. The inguinal canal: Anatomy and imaging features of common and uncommon masses. *RadioGraphics* 2008;28(3):819-835. PMID: 18480486
22. Bredella MA, Torriani M, Hornicek F, Ouellette HA, Plamer WE, Williams Z, Fischman AJ, Plotkin SR. Value of PET in the assessment of patients with neurofibromatosis type I. *AJR Am J Roentgenol*. 2007 Oct;189(4):928-35. PMID: 17885067
23. Li CS, Huang GS, Wu HD, Chen WT, Shih LS, Lii JM, Duh SJ, Chen RC, Tu HY, Chan WP. Differentiation of soft tissue benign and malignant peripheral nerve sheath tumors with magnetic resonance imaging. *Clin Imaging*. 2008 Mar-Apr;32(2):121-7. PMID: 18313576
24. Wasa J, Nishida Y, Tsukushi S, Shido Y, Sugiura H, Nakashima H, Ishiguro N. MRI features in the differentiation of malignant peripheral nerve sheath tumors and neurofibromas. *AJR Am J Roentgenol*. 2010 Jun;194(6):1568-74. PMID: 20489098
25. Mautner VF, Friedrich RE, von Deimling A, Hagel C, Korf B, Knöfel MT, Wenzel R, Fünsterer C. Malignant peripheral nerve sheath tumors in neurofibromatosis type 1: MRI supports the diagnosis of malignant plexiform neurofibroma. *Neuroradiology*. 2003 Sep;45(9):618-25. PMID: 12898075
26. Van Herendael BH, Heyman SR, Vanhoenacker FM, De Temmerman G, Bloem JL, Parizel PM, De Schepper AM. The value of magnetic resonance imaging in the differentiation between malignant peripheral nerve-sheath tumors and non-neurogenic malignant soft-tissue tumors. *Skeletal Radiol*. 2006 Oct;35(10):745-53. PMID: 16775712
27. Chee DW, Peh WC, Shek TW. Pictorial essay: imaging of peripheral nerve sheath tumours. *Can Assoc Radiol J*. 2011 Aug;62(3):176-82. PMID: 20510574
28. Chhabra A, Thakkar RS, Andreisek G, Chalian M, Belzberg AJ, Blakeley J, Hoke A, Thawait GK, Eng J, Carrino JA. Anatomic MR imaging and functional diffusion tensor imaging of peripheral nerve tumors and tumorlike conditions. *AJNR Am J Neuroradiol*. 2013 Apr;34(4):802-7. PMID: 23124644
29. Häyry P, Reitamo JJ, Tötterman S, Hopfner-Hallikainen D, Sivula A. The desmoid tumor. II. Analysis of factors possibly contributing to the etiology and growth behavior. *Am J Clin Pathol* 1982;7: 674-680. PMID: 7091047

FIGURES

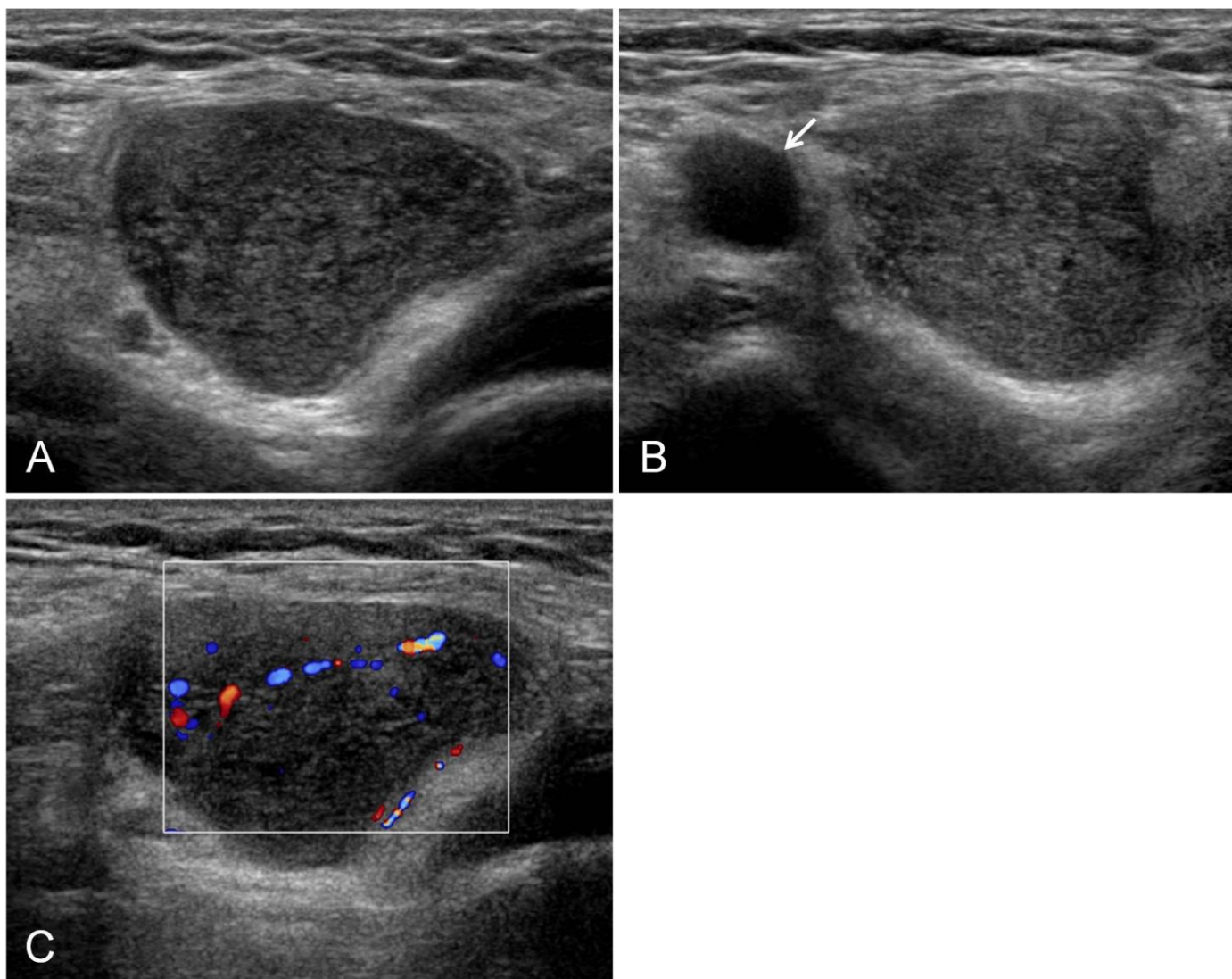


**Figure 1:** 38-year-old man with neurofibroma of the right spermatic cord. A and B: Sagittal and axial US images, respectively, through the right inguinal region demonstrate a 30 x 22 x 22 mm solid, well-demarcated, relatively homogeneous mass in the spermatic cord. The axial image (B) shows the mass is in contact with the right external iliac artery (arrow) but no vascular compression or invasion. C: Color Doppler imaging shows moderate vascularization of the mass. TECHNIQUE: US (Philips Medical Systems iU22), color Doppler, 12 MHz transducer.

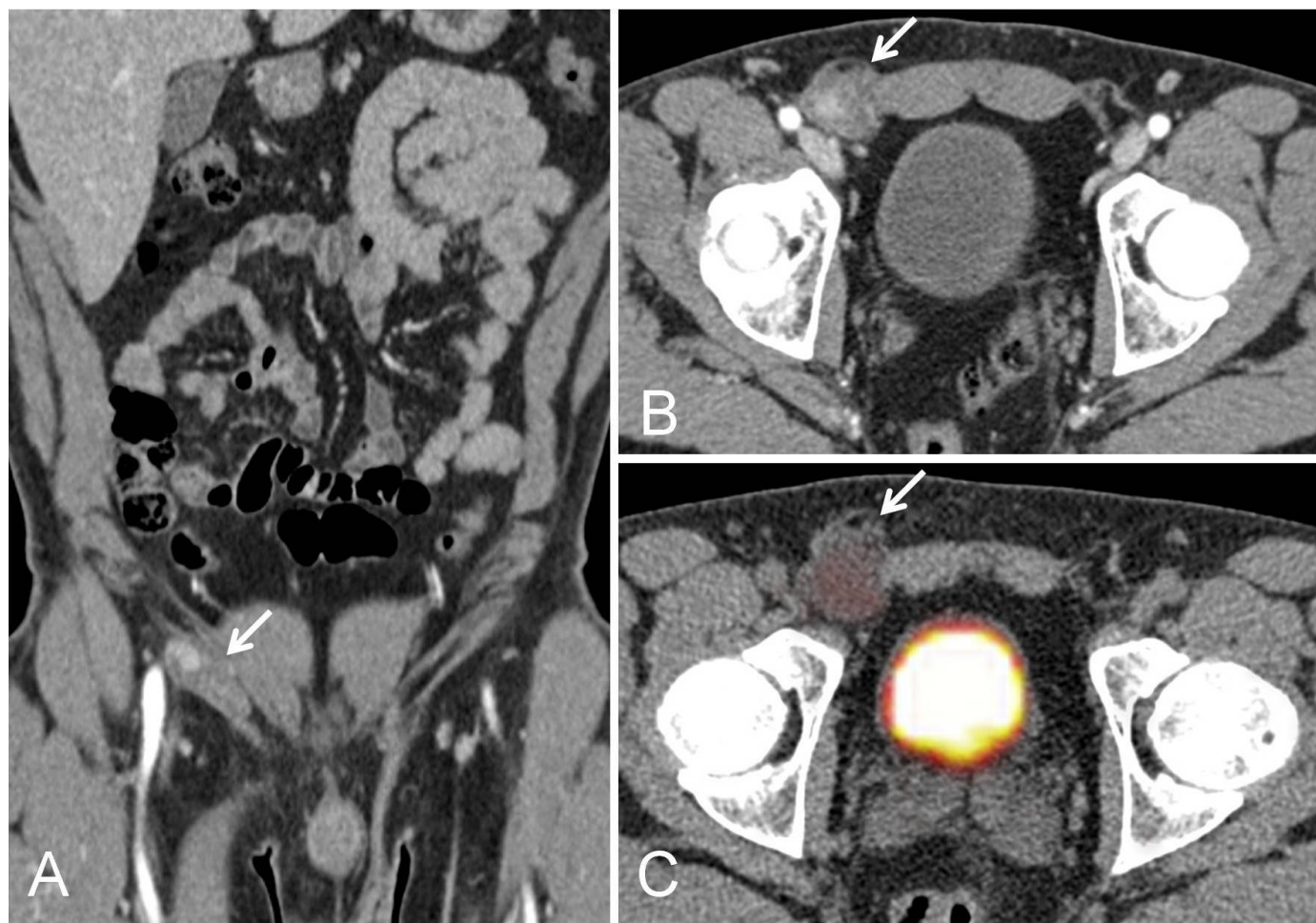


**Figure 2:** 38-year-old man with neurofibroma of the right spermatic cord. A and B: Coronal reconstruction image and axial contrast enhanced MDCT image, respectively, in the venous phase show a 41 x 32 x 30 mm well-delineated oval mass of the right spermatic cord (arrows) with heterogeneous enhancement which is more pronounced centrally. The mass is in contact with the right external iliac vessels but no vascular compression or invasion are demonstrated. C: Axial non-enhanced PET-CT fused image through the inguinal region shows the right spermatic cord mass (arrow) with only moderate uptake of the radiotracer (maximum SUV of 2.4). **TECHNIQUE:** MDCT (Siemens Biograph 64), 120 kV. Images A and B: 2 mm slice thickness, 381 mAs, 100 ml of Iohexol 350 (Accupaque® 350) contrast media. Image C: 5 mm slice thickness, 101 mAs, non-contrast, 370 MBq of 18F- FDG.

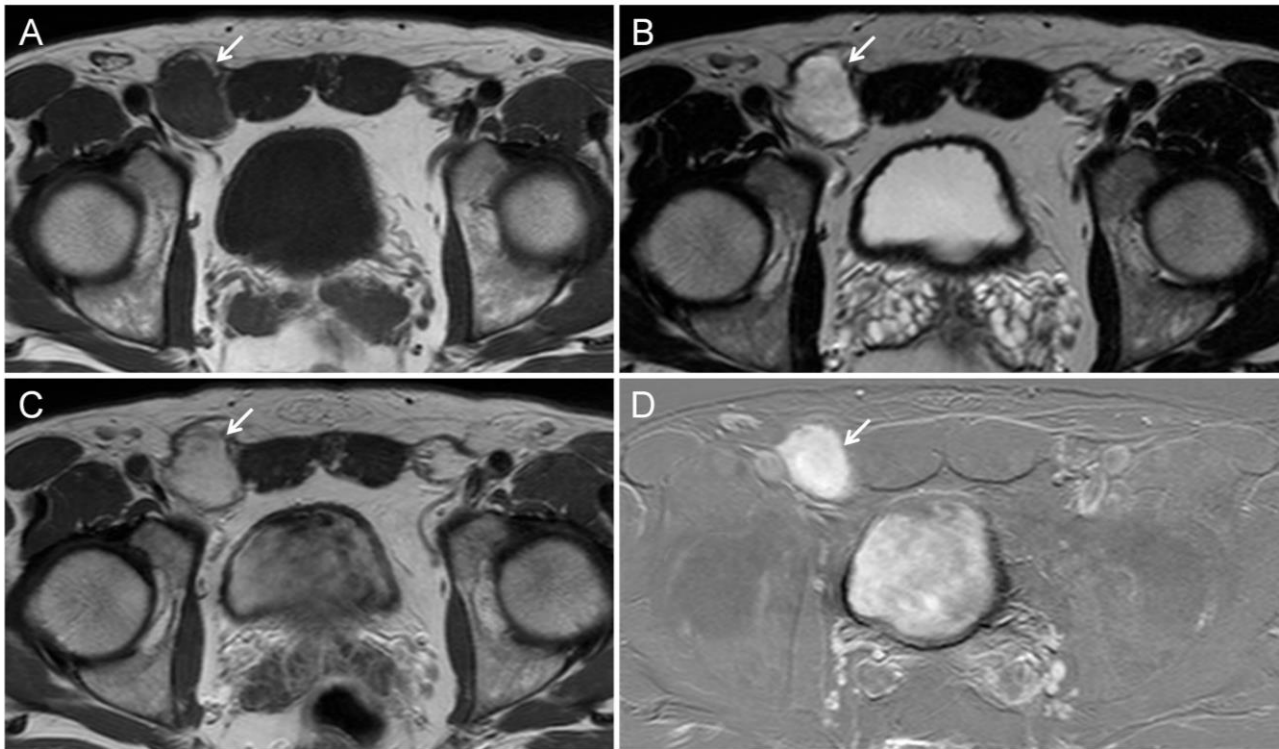


**Figure 3:** 38-year-old man with neurofibroma of the right spermatic cord. A: Axial T1W MR image through the inguinal region shows a well-demarcated homogeneous mass of the right spermatic cord (arrow) coming into contact with the right external iliac vessels without compression or invasion of the latter. The mass is nearly isointense to muscle and measures 28 x 27 mm in the axial plane. B: Axial T2W MR image shows the right spermatic cord mass (arrow) which is uniformly hyperintense to muscle and even to the surrounding fat. C and D: Axial T1W MR image after intravenous injection of gadolinium contrast media and digital subtraction image, respectively, demonstrate avid and homogeneous enhancement of the right spermatic cord mass (arrow). **TECHNIQUE:** 1.5 Tesla MRI (Philips Medical Systems Achieva), 4 mm slice thickness. Image A: TR 671.4 ms, TE 18 ms, non-contrast. Image B: TR 3974.9 ms, TE 130 ms, non-contrast. Images C and D: TR 671.4 ms, TE 18 ms, 13 ml of Gadoterate Meglumine (Dotarem®).

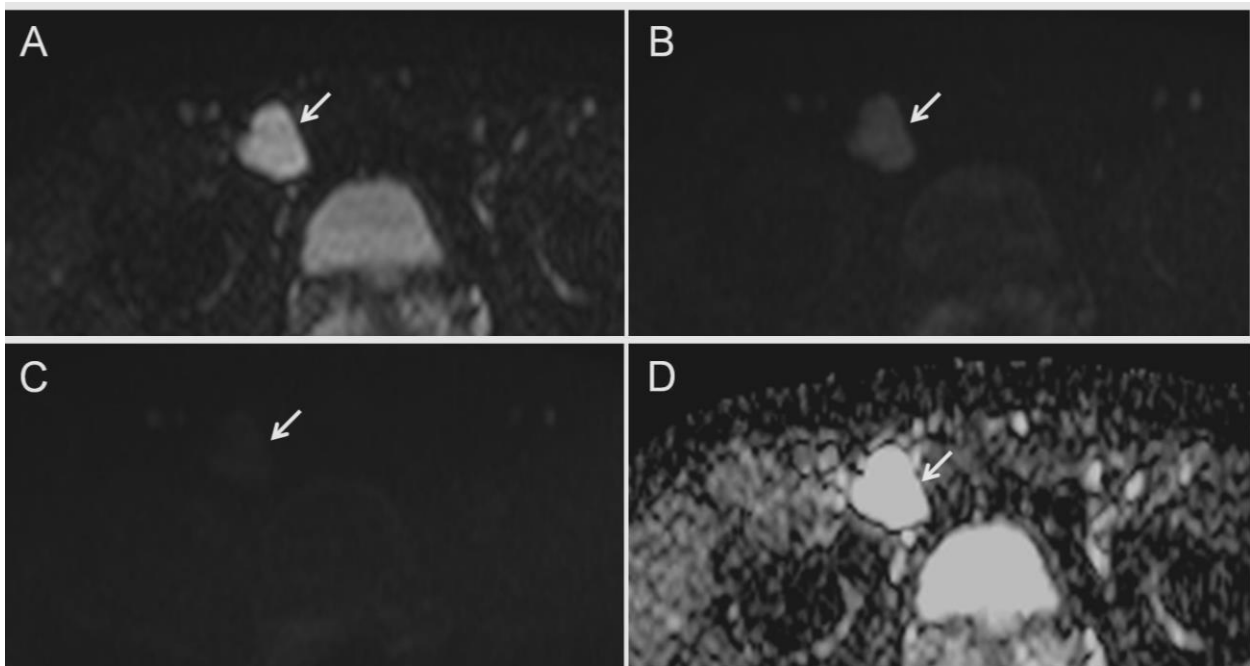


**Figure 4:** 38-year-old man with neurofibroma of the right spermatic cord. A, B and C: Axial MR diffusion-weighted imaging (DWI) at b0, b500 and b1000 (A, B, and C, respectively) through the inguinal region shows hyperintensity of the right spermatic cord mass at b0 which decreases at b500 and virtually disappears at b1000 (arrows). D: Axial MR apparent diffusion coefficient (ADC) image shows high ADC values in the lesion (arrow), which confirms an absence of water diffusion restriction. **TECHNIQUE:** 1.5 Tesla MRI (Philips Medical Systems Achieva), TR 2000 ms, TE 70 ms, 5 mm slice thickness, non-contrast.

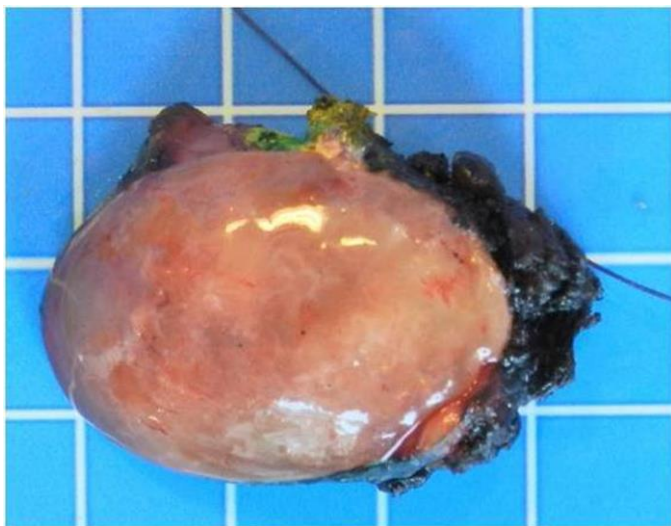


**Figure 5 (left):** 38-year-old man with neurofibroma of the right spermatic cord. Gross pathology photograph shows an oval 40 x 36 x 23 mm well-defined nodular tissue fragment weighing 13g.

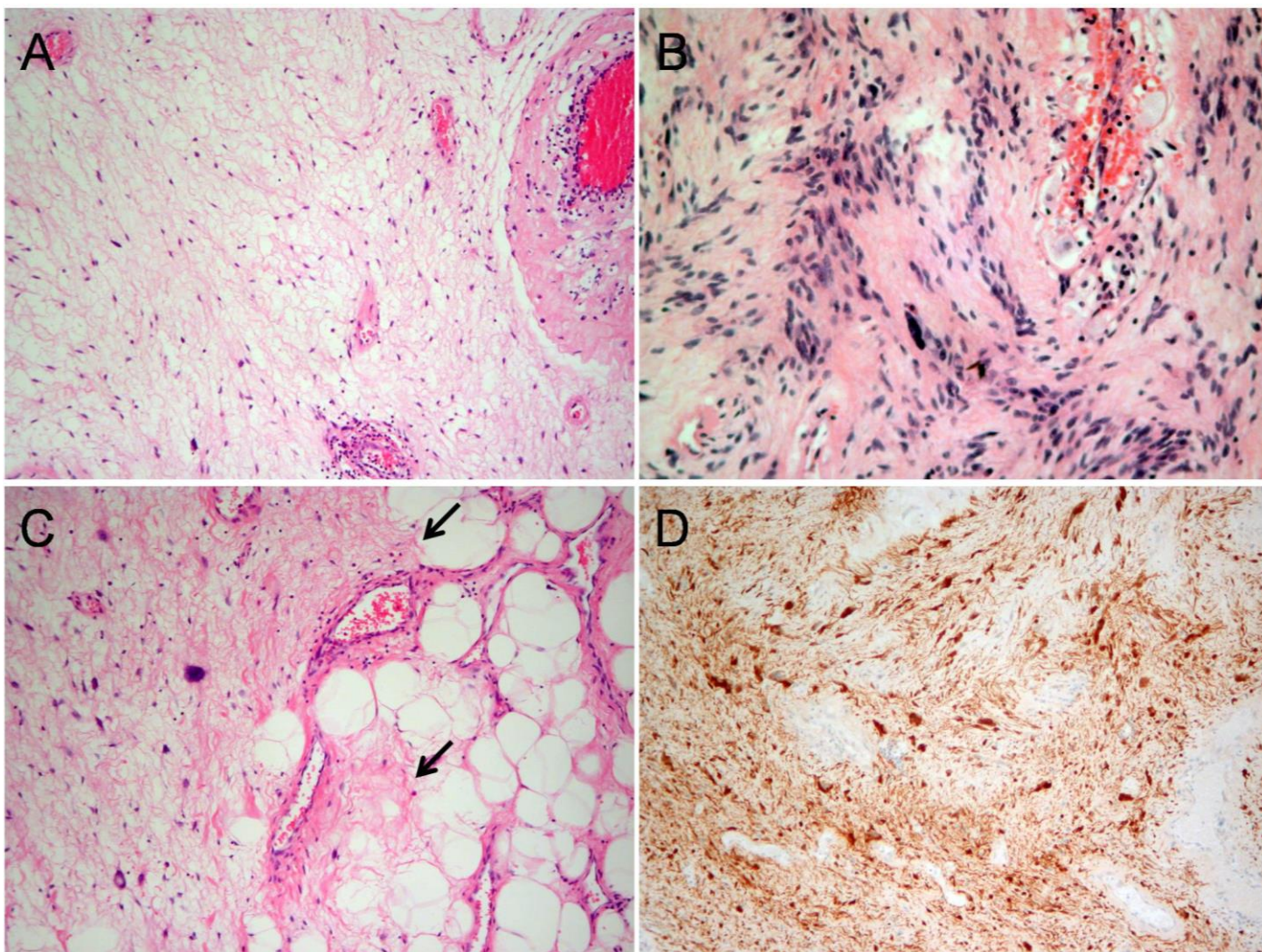


**Figure 6:** 38-year-old man with neurofibroma of the right spermatic cord. A: Micropathology photograph (x100) demonstrates multiple elongated cells with uniform oval nuclei for the most part, arranged in a lax richly vascularized fibrillary stroma. No mitotic activity is seen. B: Micropathology photograph (x200) of the central part of the lesion shows increased cellularity and a palisade-type of cellular arrangement, which are histological features of schwannoma. Again, no mitotic activity is identified. C: Micropathology photograph (x100) at the margin of the mass shows the tumor insinuating itself into the surrounding fibrofatty tissue (arrows) without destroying it. D: Immunohistochemistry photographs (x200) reveal expression of the S-100 protein by the tumor cells (seen as brown coloration).



Study	Year of publication	Tumor origin	Age (years)	Tumor dimensions (cm)
Schulte <i>et al.</i> [3]	1939	Spermatic cord	49	13 x 10 x 8
Levant and Chetlin [4]	1948	Tunica albuginea	59	1 x 0.5 x 0.3
Livolsi and Schiff [5]	1948	Intratesticular	23	9 x 7 x 4
Johnson <i>et al.</i> [6]	1975	Spermatic cord	65	5 in greatest diameter
Yamamoto <i>et al.</i> [7]	1982	Scrotum (subcutaneous)	8	5 x 1.5 x 1.5
Sánchez-Chapado <i>et al.</i> [8]	1988	Spermatic cord	66	11 x 6
Yoshimura <i>et al.</i> [9]	1990	Scrotum	41	5 x 3.5 x 3
Issa <i>et al.</i> [10]	1993	Genitofemoral nerve	77	13 x 4.5 x 3
Pelice <i>et al.</i> [11]	1994	Spermatic cord	55	8.4 (diameter)
Deliveliotis <i>et al.</i> [12]	2002	Spermatic cord	74	4 x 4 x 1
Milathianakis <i>et al.</i> [13]	2004	Spermatic cord	86	5 x 4 x 2.5
Turkyilmaz <i>et al.</i> [14]	2004	Genitofemoral nerve	14	9.5 x 7 x 4.5
Gupta <i>et al.</i> [15]	2011	Scrotum	24	10 x 9
Hosseini <i>et al.</i> [16]	2012	Spermatic cord	52	9 x 4.5
This case	2014	Spermatic cord	38	4 x 3.6 x 2.3

**Table 1:** Patients with solitary neurofibroma of the male genital tract.

<b>Etiology</b>	Benign peripheral nerve sheath neoplasm composed of Schwann cells and fibroblasts containing a rich network of collagen fibers, which arises from the genitofemoral or ilioinguinal nerve. In contrast to schwannomas they are not bound by a capsule thus allowing infiltration between the nerve fascicles.
<b>Incidence</b>	Very rare. Only 14 cases reported in the literature.
<b>Gender ratio</b>	Only men.
<b>Age predilection</b>	Occurs primarily in the first two decades of life. Reported ages are 8 to 86 (mean 49.5).
<b>Treatment</b>	Usually treated by surgical excision. However, as they are unencapsulated and infiltrate between the nerve fascicles, sacrifice of the parent nerve is necessary. This is why conservative treatment or incomplete excision are preferred in deep seated lesions or those that arise from important nerves.
<b>Prognosis</b>	Usually excellent. Malignant degeneration is very rare in the absence of NF1. Local recurrence is uncommon.
<b>Imaging findings</b>	<b>US:</b> well defined, relatively homogeneous, predominantly hypoechoic mass with poor to moderate vascularization on color and power Doppler. <b>MDCT:</b> well demarcated mass with attenuation equivalent to skeletal muscle that enhances after administration of iodinated contrast media. <b>MRI:</b> T1 isointense and T2 hyperintense to muscle. However, a hyperintense rim and central area of low signal (“target sign”) may be seen which is highly suggestive of neurofibroma. Variable enhancement pattern.

**Table 2:** Summary table for solitary neurofibroma of the male genital tract.

Entity	US findings	MDCT findings	MRI findings
<b>Solitary neurofibroma</b>	<ul style="list-style-type: none"> <li>Well defined, relatively homogeneous, predominantly hypoechoic mass</li> <li>Poor to moderate vascularisation on color and power Doppler</li> </ul>	<ul style="list-style-type: none"> <li>Well demarcated</li> <li>Attenuation equivalent to skeletal muscle</li> <li>Contrast enhancement, especially larger lesions</li> </ul>	<ul style="list-style-type: none"> <li>T1 isointense to muscle</li> <li>T2 hyperintense compared to fat</li> <li>“Target sign” is highly suggestive of diagnosis</li> <li>Contrast enhancement variable and often peripheral</li> <li>No diffusion restriction</li> </ul>
<b>Lipoma</b>	<ul style="list-style-type: none"> <li>Variable echogenicity</li> <li>Difficult to identify if unencapsulated</li> </ul>	<ul style="list-style-type: none"> <li>Well demarcated</li> <li>Low attenuation equivalent to fat</li> <li>No contrast enhancement</li> </ul>	<ul style="list-style-type: none"> <li>T1 hyperintense</li> <li>T2 hyperintense</li> <li>No contrast enhancement</li> </ul>
<b>Hematoma</b>	<ul style="list-style-type: none"> <li>Acute: low echogenicity</li> <li>Chronic: septae formation, solid appearance, calcifications</li> </ul>	<ul style="list-style-type: none"> <li>Acute: high attenuation with possibly fluid-fluid level</li> <li>Chronic: may resemble abscess</li> </ul>	<ul style="list-style-type: none"> <li>Acute: T1 isointense, T2 hypointense</li> <li>Subacute: T1 and T2 hyperintense</li> <li>Chronic: T1 and T2 hypointense</li> </ul>
<b>Abscess</b>	<ul style="list-style-type: none"> <li>Echogenic fluid collection</li> <li>Hyperechogenic capsule</li> </ul>	<ul style="list-style-type: none"> <li>Low attenuation mass</li> <li>Rim enhancement</li> </ul>	<ul style="list-style-type: none"> <li>T1 hypointense</li> <li>T2 hyperintense</li> <li>May show thin rim of contrast enhancement</li> </ul>
<b>Desmoid tumor</b>	<ul style="list-style-type: none"> <li>Homogeneously isoechoic masses</li> <li>May be mistaken for cysts</li> </ul>	<ul style="list-style-type: none"> <li>Low attenuation soft tissue mass</li> <li>Homogeneous contrast enhancement</li> </ul>	<ul style="list-style-type: none"> <li>T1 hypointense</li> <li>T2 hypointense or heterogeneous signal intensity</li> <li>Contrast enhancement</li> </ul>
<b>Liposarcoma</b>	<ul style="list-style-type: none"> <li>Variable echogenicity</li> </ul>	<ul style="list-style-type: none"> <li>Well-differentiated: mass of fat attenuation with thick septa of soft tissue attenuation</li> <li>Dedifferentiated: heterogeneously enhancing soft tissue components with calcifications</li> </ul>	<ul style="list-style-type: none"> <li>Well-differentiated: T1 hyperintense, T2 hyperintense, little contrast enhancement</li> <li>Dedifferentiated: nonspecific imaging features, heterogeneously enhancing soft tissue components</li> </ul>
<b>Burkitt lymphoma</b>	<ul style="list-style-type: none"> <li>Thickening of the spermatic cord in the inguinal canal</li> </ul>	<ul style="list-style-type: none"> <li>Thickening of the spermatic cord in the inguinal canal</li> <li>Diffuse heterogeneous enhancement</li> </ul>	<ul style="list-style-type: none"> <li>Thickening of the spermatic cord in the inguinal canal</li> <li>Diffuse heterogeneous enhancement</li> </ul>
<b>Testicular carcinoma (infiltration of the spermatic cord)</b>	<ul style="list-style-type: none"> <li>Nodular and cystic lesions in the spermatic cord</li> </ul>	<ul style="list-style-type: none"> <li>Enhancing solid components</li> <li>Nonenhancing cystic component</li> </ul>	<ul style="list-style-type: none"> <li>T1 and T2 heterogeneous signal intensity</li> <li>Contrast enhancement</li> </ul>
<b>Sarcoma</b>	<ul style="list-style-type: none"> <li>Mass infiltrating the spermatic cord</li> </ul>	<ul style="list-style-type: none"> <li>Enhancing mass infiltrating the spermatic cord</li> <li>May extend into the abdomen</li> </ul>	<ul style="list-style-type: none"> <li>Imaging findings non-specific</li> </ul>
<b>Metastases</b>	<ul style="list-style-type: none"> <li>Masses in the inguinal canal</li> </ul>	<ul style="list-style-type: none"> <li>Usually enhancing masses</li> </ul>	<ul style="list-style-type: none"> <li>T1 and T2 characteristics depend on the primary</li> <li>Usually enhancing masses</li> </ul>

**Table 3:** Differential diagnosis for solitary neurofibroma of the spermatic cord.

**ABBREVIATIONS**

18F-FDG = 2-deoxy-2-(18F)fluoro-D-glucose  
 ADC = apparent diffusion coefficient  
 CM = contrast media  
 DWI = diffusion-weighted imaging  
 HU = Hounsfield unit  
 MDCT = multidetector computed tomography  
 MRI = magnetic resonance imaging  
 NF1 = neurofibromatosis type 1  
 PET-CT = positron emission tomography-computed tomography  
 T1WI = T1-weighted imaging  
 T2WI = T2-weighted imaging  
 US = ultrasound

**KEYWORDS**

neurofibroma; spermatic cord; male genital tract; ultrasound; MDCT; MRI

**Online access**

This publication is online available at:  
[www.radiologycases.com/index.php/radiologycases/article/view/2206](http://www.radiologycases.com/index.php/radiologycases/article/view/2206)

**Peer discussion**

Discuss this manuscript in our protected discussion forum at:  
[www.radiopolis.com/forums/JRCR](http://www.radiopolis.com/forums/JRCR)

**Interactivity**

This publication is available as an interactive article with scroll, window/level, magnify and more features.  
 Available online at [www.RadiologyCases.com](http://www.RadiologyCases.com)

Published by EduRad



[www.EduRad.org](http://www.EduRad.org)